

- Journal of Materials Science*. Vol.45, No 19, p.p. 5150 -5157.
10. Lu H. M., Jiang Q. (2005). Surface Tension and Its Temperature Coefficient for Liquid Metals. *J. Phys. Chem. B*. Vol.109, p.p. 15463 -15468.
  11. Naidich Yu.V., Kolesnichenko G.A., Lavrinenko I.A., Motsak Ya.F. *Pajka i metallizacija sverhtverdyh instrumental'nyh materialov* [Brazing and metal coating of super hard instrument materials]. Kiev, Naukova dumka, 1977, p.186.
  12. Popel S.I. *Teoriya metallurgicheskikh processov* [Theory of metallurgical processes]. Moscow, VINITI, 1971, p.132



## Forming Process of Automotive Body Panel based on Incremental Forming Technology

**Guangcheng Zha<sup>1,2</sup>, Jinbo Xu<sup>3</sup>, Xiaofan Shi<sup>1,2</sup>, Xun Zhou<sup>1</sup>, Chuankai Lu<sup>1</sup>**

<sup>1</sup> *School of Materials Science and Engineering, Nanjing Institute of Technology, Nanjing 211167, Jiangsu, China*

<sup>2</sup> *Jiangsu Key Laboratory of Advanced Structural Materials and Application Technology, Nanjing 211167, Jiangsu, China*

<sup>3</sup> *Nanjing Research and Development Center, Engineering Technology Associates Inc, U.S, Nanjing 210015, Jiangsu, China*

### Abstract

Development of new vehicle model is a long-time and high-cost procedure traditionally. In this paper, the typical automotive body panel has been formed by means of Single Point Incremental Forming (SPIF) technology which is high-flexibility, short-cycle, low-cost and so on. Based on the stereolithography (STL) triangle meshes, the SPIF main direction of the automotive body panel has been determined. In accordance with the partial fracture on the panel concave surface, the forming principles on single-stage and double-stage have been analyzed. Multi-stage forming has been applied to realize the automotive panel processing successfully. To ensure the SPIF efficiency and quality, the first-stage forming process has been to finish the preliminary integral forming for the parts according to the concave intermediate shape, and then to conduct the second-stage forming for the concave final shape locally. The experimental data has showed that the reasonable forming stage can effectively optimize the thickness distribution of the parts. It is helpful to new vehicle development based on the SPIF flexible manufacturing technology in the future.

Key words: AUTOMOTIVE BODY PANEL, SINGLE POINT INCREMENTAL FORMING, MULTI-STAGE FORMING, THICKNESS DISTRIBUTION

**1. Introduction**

Manufacturing of new vehicle body panel often requires complicated process including mold design, soft mold manufacturing, test modification, die commission and so on. The trail-produce of a new panel part usually takes 4 to 6 months. Currently in China, new automotive body panels are commonly hand-made by experienced fitters during prototype vehicle trail-producing, the dimensional accuracy and surface quality cannot meet the requirements well.

The Single Point Incremental Forming (SPIF) is a flexible non-molding forming technology based on the layered manufacturing method of rapid prototyping technology. The complicated SPIF digital model is dispersed into a series of 2D section layers along the Z axis (height), and the envelope surface formed by the trajectory of the forming tooling head replaces the surface of the mold. Compares to the traditional mould forming, SPIF technology can significantly increase sheet metal forming limit and comes with advantages such as high flexibility, lost cost and high efficiency[1-5]. And since it only requires a simple support-body, the manufacturing cycle of the automotive part can be shortened to 1-2 months or less, especially applicable for new vehicle model development or small batch production.

Automotive body panel has complex shape which makes the forming process is far more complicated than common sheet metal parts. According to the thickness law of cosines  $t = t_0 * \cos \theta$  during the incremental sheet forming[6], the parts will fail to be

formed successfully when the local forming angle  $\theta$  exceeds the limit forming angle  $\theta_{max}$ . The reasonable forming main direction should be determined according to the parts shape. The appropriate forming process need be optimized firstly based on the local difficulty-forming characteristics.

This paper has finished the SPIF experimental processing for a typical automotive body panel. According to the difficulty-forming characteristics of the parts, the strategy of multi-stage deformation was applied on the local areas on the basis of integral forming preliminary. The experimental samples have been measured and preliminarily analyzed in the end.

**2. Experimental conditions**

The special-purpose Single Point Incremental Forming machine NH-SK1060, designed by Nanjing Aeronautical Institute and Sikai Limited company, was adopted as the experimental equipment. Processing range is 600mm x 1000mm, feeding speed is 1~18000mm/min, speeds of the three axes are X = 25m/min, Y= 25m/min, Z=20m/min. To achieve the positive forming process, an A axis is added into the system to realise the motion of support-body based on the X, Y and Z three-axis linkage.

The experimental material adopted the galvanised sheet DX54D+Z which is usually used to manufacture automotive interior and external panel, structural part and reinforcement part. The main chemical composition and mechanical properties are shown in Table 1.

**Table 1.** Composition and performance parameters of H180YD+Z

Chemical composition						Mechanical properties			
C	Si	Mn	P	S	AiT	Yield strength (MPa)	Tensile strength (MPa)	Elongation	Yield ratio
≤0.04	≤0.5	≤1.5	≤0.06	≤0.025	≥0.02	≥180	≥340	≥34	≥0.5~0.6

**3. Forming experiment**

**3.1. Construction of experimental model**

The automotive body panel has been selected as experimental object shown in figure 1. Considering the processing range and forming efficiency of the NH-SK1060, the dimensions of this part are reducibly scaled by 1:5. There are some difficulty-forming features such as reinforcing ribs and groove wall, and holes to exist on the part digital model. After trim these features accordingly, the incremental forming

model was shown in figure 1. The trimmed areas will be processed by subsequent handling afterwards.

There is a notching hole on one side of the automotive body part profile and an evenly closed loop is almost impossible to form with incremental forming tool track. Also because the internal stress accumulated on the part would easily cause instability, necessary addendum surface and clamping surface should be added into the model. Finally, the adding addendum surface CAD model is shown in Figure 2.

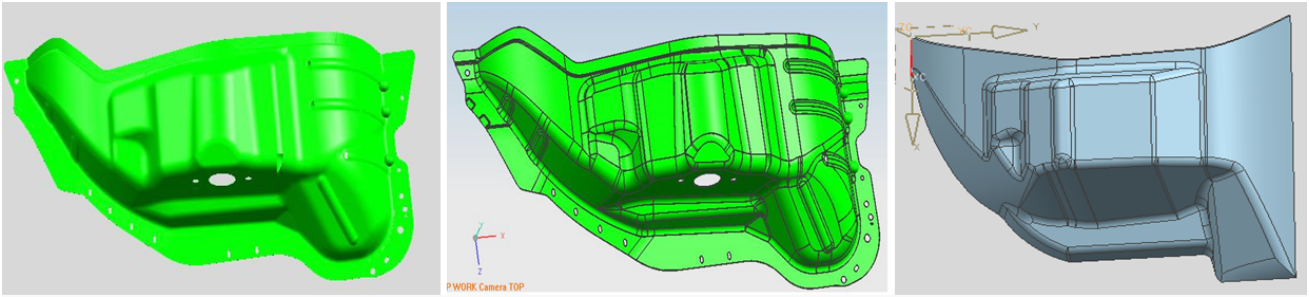


Figure 1. Model for SPIF experiment

3.2. Experiment process

The part thickness during incremental forming follows the law of cosines  $t = t_0 * \cos \theta$  [6] (the forming angle  $\theta$  is the angle between the normal vector of the processing position and the z-axis). Whether the part can be formed smoothly is directly determined by the placement of that part, aka the main forming direction. The main direction selected should ensure that the forming angle  $\theta$  at any position of the

parts is less than the forming limit angle  $\theta_{max}$ . The thickness of each part of the parts should be uniform even as far as possible at the same time, that means the differences of the forming angles should not be too big. Traditional main forming direction decision depends on experience. It's very difficult to achieve ideal forming position. This paper will adopt the part STL model to determine the incremental main forming direction [7].

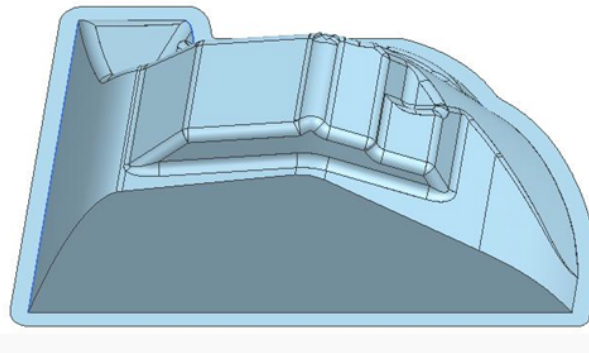


Figure 2. Adding addendum surface

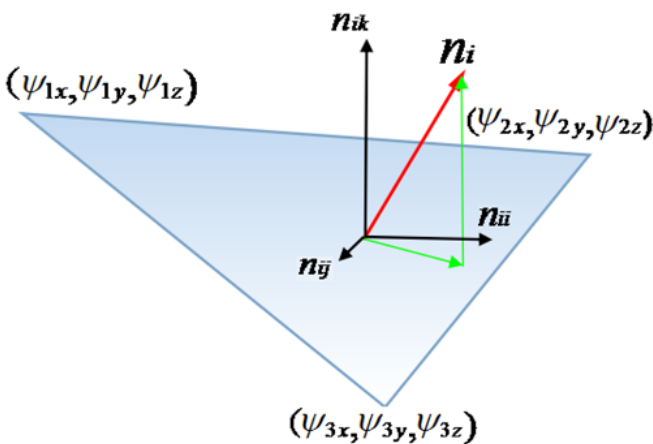


Figure 3. Triangle mesh diagram

The idea is to discrete the digital part model into STL triangle meshes under certain accuracy. As shown in Figure 3, the unit of STL triangle meshes includes the coordinate value of three vertices, namely,  $\psi_{ik}$ ,

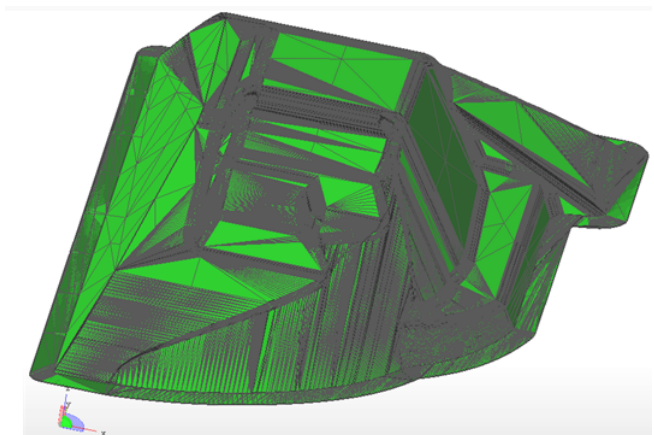
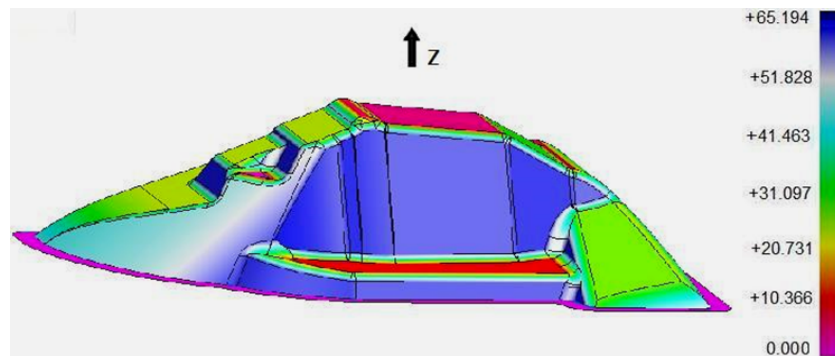


Figure 4. STL model of the part

$\psi_{iy}$ ,  $\psi_{iz}$  ( $i = 1, 2, 3$ ), and the normal vector  $n_i$  of the triangle mesh selected, in which  $n_{iu}$ ,  $n_{ij}$ , and  $n_{ik}$  are the components of  $n_i$  along the directions of the x-, y-, and z-axes, respectively. The normal vec-

tor of optional position on the parts surface could be replaced by the normal vector of the triangle mesh selected. The angle between the normal vector and the z-axis can be regarded as the forming angle  $\theta$  of

this position. In accordance with the the forming limit angle  $\theta_{\max}$  and the forming angle  $\theta = \arccos(t_i/t_0)$  ( $t_0$  is the initial sheet thickness) based on the specified



**Figure 5.** Cloud charts of forming angles

thickness  $t_i$  in advance, of the parts can be determined with the law of cosines for parts that require special thickness  $t_r$ . Triangle mesh is selected in this position, and the angle between the normal vector of the mesh and the z-axis is generated to reach  $\theta$  after rotation. The final vertex coordinates of each triangular mesh can be obtained via the rotation matrix, and the STL model spatial position is the processing position of the part[7]. Figure 4 is the obtained STL model of the body panel by setting the triangle tolerance and the adjacent tolerance as 0.1. The cloud chart of the main forming direction after rotate-vector optimization was shown in Figure 5 .

The experimental results shows that the maximum forming angle  $\theta_{\max}$  of the 0.7mm DX54D+Z sheet metal is approximate  $70^\circ$ . As shown in Figure 5, the largest forming angle  $\theta$  of the parts fell within the limit forming angle  $\theta_{\max}$ . The automotive body panel can be formed theoretically. Figure 6 is the support-body for positive forming process.

The experimental chose a piece of DX54D+Z sheet metal of the size 250 x 250 x 0.7mm, chose a 40Cr 10mm semi-sphere tool bit, hardness is 58-60HRC, the tooling speed was set at 180mm/min, feed rate is 0.15mm, uses common lubricant.

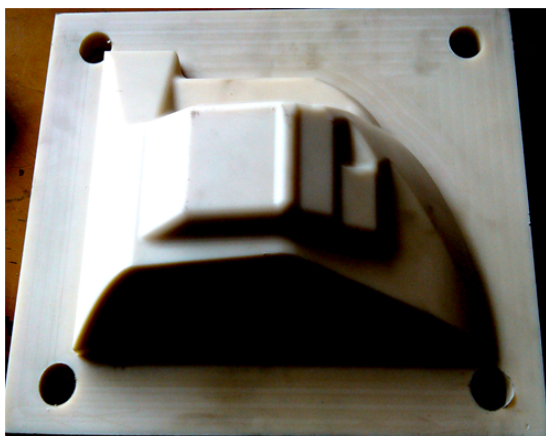


**Figure 6.** Support-body

As shown in figure 8, the formed sample rupture at the yellow concave area as figure 9 . Even though this area can be formed theoretically according to the cloud model as Figure 5, the forming angle of the concave back wall was reaching the limit. forming

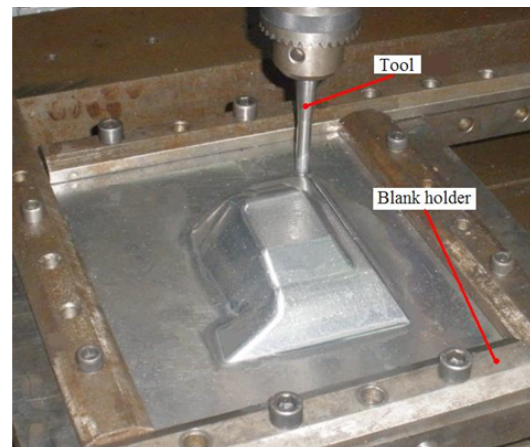


**Figure 7.** Parts forming process

angle  $\theta_{\max}$ . Also, unreasonable tooling head feeding rate, tool track and lubricant condition can also cause rupture in the actual increment forming process. At the same time, according to the thickness cosine law, even if the part

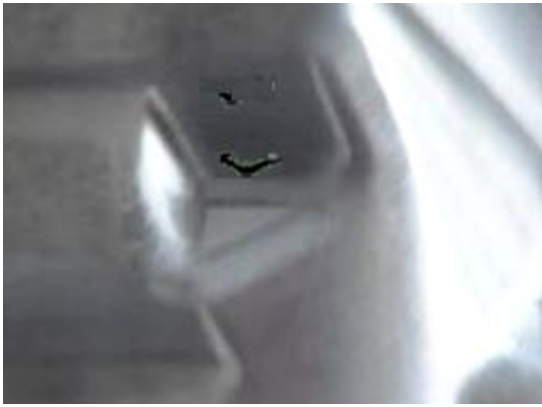


Figure 8. Fracture of the single-stage forming part

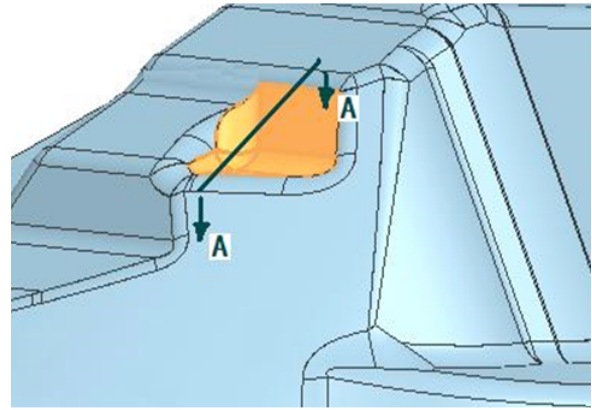


Figure 9. Schematic diagram of fracture position

would not rupture when the forming angle  $\theta$  was rather larger, the heavily reduced thickness can also affect the strength and stiffness of the part. Young [8], M.Skjoedt[9] and Iseki [10] have proposed that adding appropriate forming stage could effectively improve the sheet forming limit [11]. Multi-stage forming is one of the most practical solutions to avoid severe thinning in SPIF. As shown in figure 10, the a and b respectively indicate the different schematic diagram of single-stage and double-stage forming.

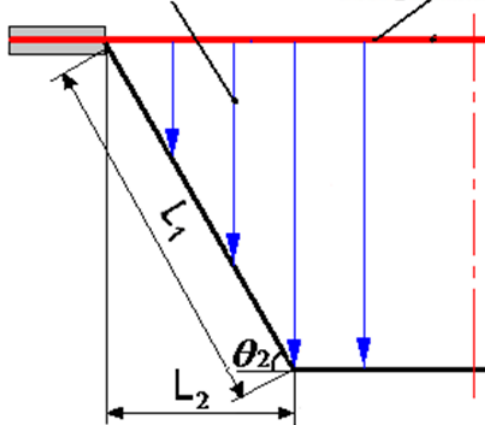
As shown in figure 10a, single-stage incremental

forming follows the law of cosines. The maximum principal strain based on the shear deformation principle of the forming plate is:

$$\varepsilon_{major1} = \ln \frac{L_2}{L_1} = \ln \sec \theta_2 \quad (1)$$

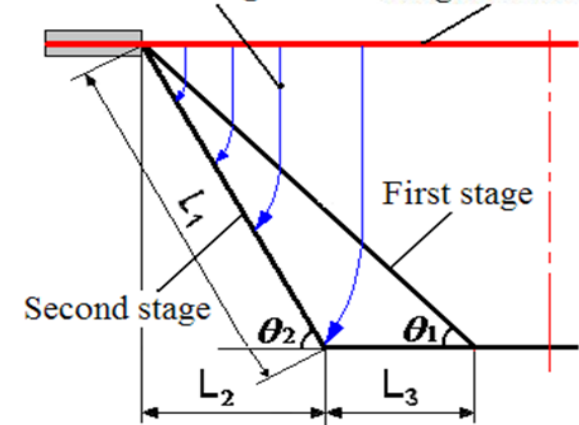
Obviously, the sheet thinning rate is proportional to the forming angle  $\theta_2$ . When  $\theta_2$  is rather big or even equals to  $90^\circ$ , the ultimate thickness will be impossible to meet the requirement by using single-stage forming method.

Material flowing traces Original Sheet



a) single-stage

Material flowing traces Original Sheet



b) Double-stage

Figure 10. Forming principles for different stages

According to the double-stage principle shown in figure 10 b, unlike a single-stage forming whose tool path is directly generated from  $\theta_2$ , a double-stage process will achieve the final part through one inter-

mediate shape[12], which represents a first-stage forming with forming angle  $\theta_1$ . The maximum principal strain for the double-stage on this sheet metal will be:

$$\varepsilon_{major2} = \ln \frac{(L_1 + L_3)}{(L_2 + L_3)} = \ln \left( \frac{\tan \theta_1}{\sin \theta_2} + 1 - \frac{\tan \theta_1}{\tan \theta_2} \right) \quad (2)$$

The  $\varepsilon_{major1}$  and  $\varepsilon_{major2}$  respectively represent the principal strains of single-stage forming and double-

stage forming. According to the formula(1), (2) it is easy to deduce the formula:

$$\Delta \varepsilon_{major} = \varepsilon_{major1} - \varepsilon_{major2} = \ln \frac{L_1 L_2 + L_1 L_3}{L_1 L_2 + L_2 L_3} \quad (3)$$

It is evident that  $L_1 > L_2$ , so  $\Delta \varepsilon_{major} \geq 0$ . Namely, the thickness reduction using a double-stage

forming is smaller than that which uses a single-stage process. Therefore, if it is difficult to meet the requirements of the sheet thickness with a single-pass forming, it is effectual to change the forming stage.

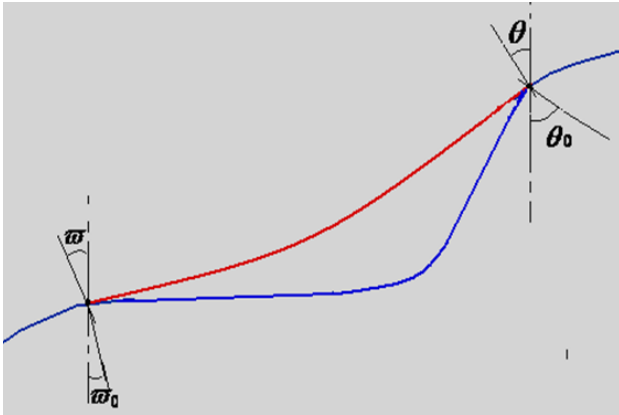


Figure 11. Transitional surface section for A-A

To avoid the concave rupture of automotive body panel, we change the forming method for this area from single-stage to double-stage without changing its main forming direction. To ensure the processing efficiency and forming quality, the first-stage forming process was to finish the preliminary integral forming for the panel according to the concave intermediate shape, and then to conduct the second-stage forming for the concave area locally. The feed rate of the first-stage forming and the second-stage forming were respectively set to 0.15mm and 0.1mm.



Figure 12. Concave formed by double-stage

The Figure 11 is the concave position A-A profile view of Figure 9, the starting single-stage forming angle is  $\theta=65^\circ$ , the ending forming angle is  $\omega_0=10^\circ$ . In this double-stage forming process, the first-stage forming obtains the blending surface, set the starting forming angle as  $\theta=35^\circ$ , and to ensure the smooth transition between the blending surface and its outline, set the ending forming angle as  $\omega=20^\circ$ . The concave area was smoothly formed, as shown in Figure 12, after the above process adjustments. Figure 13 shows the integral part.

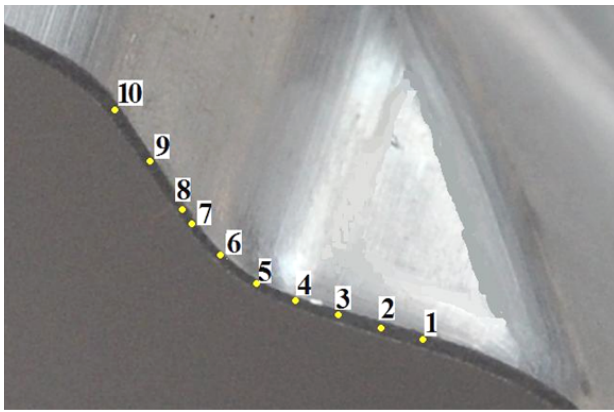


Figure 13. Forming part

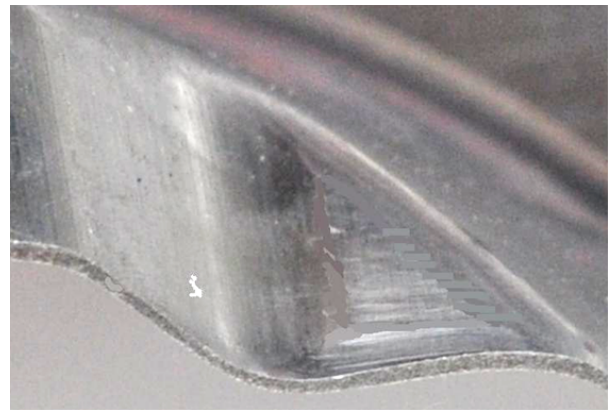
### 3.3. Thickness analysis of the formed parts

The formed parts of different forming stage have been cut along the concave A-A profile view shown in Figure 9. The sectional view of the parts is shown

in Figure 14. The points selected to measure have been shown in Figure 14a and the thickness data of the parts have been shown in Table 2.



a) Double-stage



b) Single-stage

Figure 14. Section view of parts for different stage

As shown in Table 2 and Figure 15, there are deviations between the actual thickness and theoretical thickness of single-stage forming, but generally the thickness is in accord with the cosine law  $t = t_0 * \cos \theta$ . Compared with the single-stage

forming, the thickness distribution of the double-stage formed part is more uniform. This shows that reasonable multi-stage SPIF can improve the thickness distribution of the formed part.

Table 2. Section thickness of parts for different stage

Measuring points	Theoretical forming angle(°)	Theoretical thickness of one-stage (mm)	Actual thickness of one-stage (mm)	Thickness Error of one-stage(%)	Actual thickness of double-stage (mm)
1	10	0.689	0.684	-0.73	0.617
2	10	0.689	0.675	-2.04	0.621
3	10	0.689	0.653	-5.23	0.613
4	27	0.623	0.645	3.53	0.566
5	40	0.536	0.494	-7.84	0.523
6	68	0.262	0.289	10.3	0.413
7	70	0.239	0.202	-15.49	0.421
8	70	0.239	0.225	-5.86	0.446
9	70	0.239	0.245	2.51	0.457
10	70	0.239	0.25	4.6	0.468

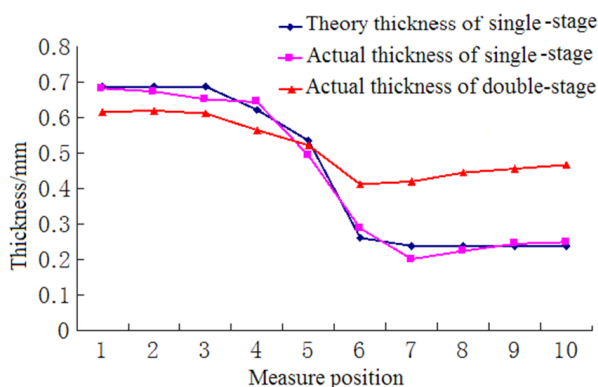


Figure 15. Thickness curve for forming parts

#### 4. Conclusions

Complicated structural parts can use the integral forming combined with local multi-stage forming process. The difficulty-forming position of the parts

can be effectively formed smoothly. The material thickness of the single-stage SPIF formed part is generally accord with cosine law. The reasonable multi-stage forming process could improve the thickness distribution of the formed part.

#### Acknowledgements

This work is supported by Innovation Fund Project for Nanjing University of Technology. (Project No. CKJB201304, CKJB201402, YKJ201311, and YKJ201404).

This work is supported by the Opening Project of Jiangsu Key Laboratory of Advanced Structural Materials and Application Technology. (Project No. ASMA201410 and ASMA201417).

This work is supported by Students Innovation Project of Jiangsu Province. (Project No. 201511276041Y).

### References

1. Malhotra R, Reddy NV, Cao J.(2010) Automatic helical toolpath generation for single point incremental forming. *J Manuf Sci E-T ASME*, 132(6), p.p.98-101.
2. Jackson KR, Allwood JM, Landert M . (2008) Incremental forming of sandwich panels. *J Mater Process Technol*, 204(1-3), p.p.290-303.
3. Micari F, Ambrogi G, Filice L. (2007) Shape and dimensional accuracy in single point incremental forming: state of the art and future trends. *J Mater Process Technol*, 191(1), p.p.390-395.
4. Bambach M, Taleb Araghi B, Hirt G. (2009) Strategies to improve the geometric accuracy in asymmetric single point incremental forming. *Prod Eng Res Devel*, 3(2), 145-156.
5. Hagan E, Jeswiet J.(2003) A review of conventional and modern single-point sheet metal forming methods. *Proc I Mech E Part B J Eng Manuf* , 217(2), p.p.213-225.
6. Hirt G, Ames J, Bambach, et al. (2004)Forming strategies and process modeling for CNC incremental sheet forming. *CIRP Annals-Manufacturing Technology*, 53(1), p.p. 203-206.
7. Guangcheng Zha, Xiaofan Shi and Wei Zhao, et al. (2015) Optimization of and Experiment on the Main Direction of Incremental Forming. *Metallurgical and mining industry*, 7(8), p.p.219-227.
8. Young D, Jeswiet J .(2004) Wall thickness variations in single-point incremental forming. *Proc IMechE Part B: J Eng Manuf*, 218(11), p.p.1453-1459.
9. M. Skjoedt, N. Bay, B. Endelt. (2008) Multi Stage Strategies for Single Point Incremental Forming of a Cup. *Int J Mater Form*, 1(1 Supplement) , p.p.1199-1202.
10. Iseki, Naganawa (2002) Vertical Wall Surface Forming of Rectangular Shell Using Multi-stage Incremental Forming with Spherical and Cylindrical Rollers. *Journal of Materials Processing Technology*, 130(02), p.p.675-679.
11. Kim TJ, Yang DY . (2000)Improvement of formability for the incremental sheetmetal forming process. *Int JMech Sci* , 42(7), p.p.1271-1286.
12. Junchao Li, Pei Geng, Junjian Shen (2013) Numerical simulation and experimental investigation of multistage incremental sheet forming. *Int J Adv Manuf Technol*, 68(9-12), p.p.2637-2644.

## Metallurgical and Mining Industry

[www.metaljournal.com.ua](http://www.metaljournal.com.ua)